

# Simulation Study of Various Layers and Double $\delta$ -Doping Effect on Device Performance of InAlAs/InGaAs/InP HEMT

A. B. Khan<sup>a\*</sup>, S. G. Anjum<sup>a</sup> and M. J. Siddiqui<sup>b</sup>

<sup>a</sup>Research Scholar, Department of Electronics Engineering, Z. H. College of Engineering & Technology AMU, Aligarh-202002

<sup>b</sup>Professor, Department of Electronics Engineering, Z. H. College of Engineering & Technology AMU, Aligarh- 202002

Corresponding author: email: aboobakar.rs@amu.ac.in

Received date: November 11, 2016; revised date: June 13, 2017; accepted date: June 14, 2017

## Abstract

The InAlAs/InGaAs/InP HEMT (High Electron Mobility Transistor) lattice matched to InP offers outstanding high frequency, low noise operation for low-noise amplifiers. In this work, efforts have been made to study and optimize the device performance of 0.5  $\mu\text{m}$  gate length double  $\delta$ -doped InP-based In<sub>0.53</sub>Ga<sub>0.47</sub>As/In<sub>0.52</sub>Al<sub>0.48</sub>As HEMT with the help of the variation of various parameters like  $\delta$ -doping, Schottky layer thickness, spacer layer thickness and gate length. To study the impact of various parameters we use Atlas Silvaco TCAD numerical simulation tool. We have performed characterization studies of two-dimensional electron gas (2DEG) in the channel layer, conduction band discontinuity ( $\Delta E_C$ ), transconductance ( $g_m$ ), threshold voltage ( $V_{th}$ ) and cut-off frequency ( $f_T$ ) to optimize the device performance. And hence optimize figure of merit such as transconductance and cut-off the frequency of the device.

**Keywords:** mobility;  $\delta$ -doping; 2DEG; transconductance; threshold voltage; cutoff frequency.

## 1. Introduction

InAlAs/InGaAs/GaAs III-V Ultrafast technology of MODFET (modulation doped field effect transistor) device is used in MMIC (monolithic microwave integrated circuits) for high-speed [1-3]. Today the GaN-based HEMT are used for power devices with low on-state resistance [4-7]. But in communication and various types of equipment's varying from electronic wafer systems to cell phones likes radio astronomy and radar InAlAs/InGaAs HEMT plays a key role. Numerous technologies are nowadays based on InGaAs/InAlAs quantum well HEMT devices [8-9]. These applications [10] are exposed to large sheet carrier density in the 2DEG quantum well and higher transport properties of InGaAs which is formed near heterointerface [11-12]. But the limitation of the InP-based HEMT's impacts ionization effects, which occur in InGaAs narrow band gap channel layer. A number of negative consequences to improve the impact ionization effects likes decreased the breakdown voltage of on state and off state, there is in kink effects, output conductance and lasting device degradation. Due to higher impact ionization effects in the narrow band gap channel, conventional In<sub>0.53</sub>Ga<sub>0.47</sub>As HEMT's bear low breakdown voltage.

The InAlAs/InGaAs/InP HEMT lattice matched to InP offers outstanding low noise, high-frequency operation for low-noise amplifiers. In this article, works have been done to simulate and optimize the performance of 0.5  $\mu\text{m}$  gate length double  $\delta$ -doped InP-based In<sub>0.53</sub>Ga<sub>0.47</sub>As/In<sub>0.52</sub>Al<sub>0.48</sub>As HEMT with the help of the

variation of various parameters like  $\delta$ -doping, Schottky layer thickness, spacer layer thickness and gate length. To get the effect of numerous parameters TCAD Silvaco Atlas numerical simulation tool has been used. In this simulation, various important device parameters like the high electron density of two-dimensional electron gas (2DEG), conduction band discontinuity ( $\Delta E_C$ ), transconductance ( $g_m$ ), threshold voltage ( $V_{th}$ ) and cutoff frequency ( $f_T$ ) have been obtained. Further, the effect of parameter variation on the high electron density (2DEG), conduction band discontinuity and optimization of the performance of HEMT has been analyzed. These values, then used to optimize the figure of merit such as cutoff frequency and transconductance of the device.

## 2. Device Structure

The InAlAs/InGaAs HEMT device schematic cross-section view is Fig.1. The structure of this device has InGaAs cap layer which is heavily doped with Si at approximately  $10^{18}/\text{cm}^3$ , offers a good ohmic contact to the HEMT. The cap layer not only decreases the drain and source contact resistance of the device but also protect the surface depletion and oxidation of the Schottky layer. This device structure also consists a wide bandgap Schottky layer than the channel layer material. At the InAlAs/InGaAs heterointerface, a large conduction band discontinuity occurs due to this the free electrons diffuse from higher bandgap InAlAs material into lower bandgap InGaAs channel layer and form 2DEG. Due to this a high carrier concentration is obtained into the channel layer.

An InAlAs thinner Schottky layer makes the possible small distance

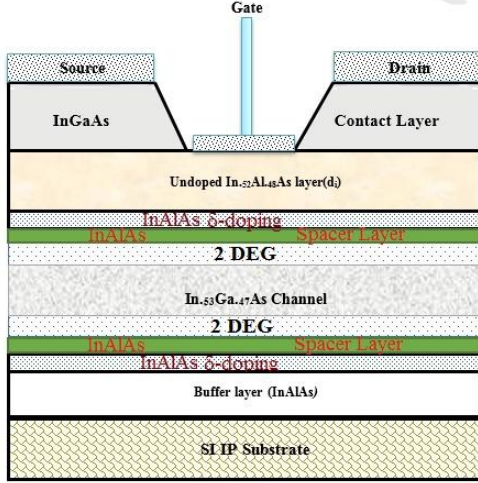


Figure 1: InP-based HEMT model

between the gate metal and the channel layer, which provide high transconductance but decreases the breakdown voltage of the device.

The spacer layer separates the ionized donors and 2-DEG at the heterointerface of donor layer and the channel layer. It also decreases Coulomb scattering of the donor atoms due to this enhance the electron mobility of the device. The thickness of the doping layer is the order of 3 Å with a very high doping concentration of  $2 \times 10^{18}/\text{cm}^3$ , supply all the electrons into the channel layer and form 2DEG. This device consists two doping layer which serves as the source of electrons. Because the device consists two doping layers so it is called double  $\delta$ -doped HEMT. Due to double doping electron transfer from both side and form 2DEG into the channel layer.

### 3. Physical Model of HEMT

The basic qualitatively description of HEMTs operation is based on one-dimensional charge control model and the direction of charge control model is perpendicular to the heterointerface. The electron wave function satisfies the Schrodinger equation while the electric potential (band diagram) and charge distribution follow the Poisson equation. Theoretically, by self-consistently solving the two equations the charge profile and the potential can be calculated. Based on the assumption that the carrier transfer from the supply layer is confined in the 2DEG, across hetero-interface the Fermi level is constant, and the potential well at the channel can be approximated by a triangular well, the electron charge ( $n_s$ ) stored at the interface in a modulation doped structure is [13]

$$n_s = \frac{\epsilon}{qd} [V_g - (\Phi_b - V_{p2} + \frac{E_{fi}}{q} - \frac{\Delta E_C}{q})] \quad (1)$$

where  $\Phi$  is barrier layer dielectric constant,  $q$  is electron static charge,  $d$  is the sum of the thickness of the doped barrier  $d_i$  and Undoped barrier  $d_d$ ,  $\Phi_b$  is the Schottky barrier height of the gate metal deposited on the barrier layer,  $V_g$  is the applied gate to source voltage,  $V_{p2} = \frac{qN_d d_i^2}{2\epsilon}$  while  $N_d$  is the donor concentration in the barrier layer,  $\Delta E_C$  is the conduction band offset between the channel and barrier and  $E_{fi}$  is the Fermi level with respect to the conduction band edge in the channel layer.

The interface change in eqn-1 can be expressed in a more general form which can be used for the planar doped structure as [14]:

$$n_s = \frac{\epsilon}{q} \frac{V_g - V_{th}}{d_B + d_s + \Delta d} \quad (2)$$

where  $d_B$  and  $d_s$  are the thickness of the barrier and spacer layer respectively,  $\Delta d$  is the average distance between 2DEG and interface. The threshold voltage is given as:

$$V_{th} = \Phi_B - \frac{\Delta E_C}{q} - V_{p2} \frac{E_{fi}}{q} \quad (3)$$

for modulation doped structure

$$V_{th} = \Phi_B - \frac{\Delta E_C}{q} - \frac{\epsilon}{q} N_d d_B \quad (4)$$

for  $\delta$  doped structure.

$g_m$ , the transconductance is defined as the change in the drain to source current divided by the change in the gate to source voltage at certain drain to source voltage:

$$g_m = \frac{dI_d}{dV_g} | V_{ds} = \text{constant} \quad (5)$$

It is the most important dc figure of merit in field effect transistors as it demonstrates the current modulation efficiency of the gate.

The current cut-off frequency  $f_T$  is defined as the frequency at which current gain of a two-port network goes to unity. It is the maximum frequency the device can work for current amplification. Under the assumption that feedback capacitance is negligible in HEMTs,  $f_T$  is given by:

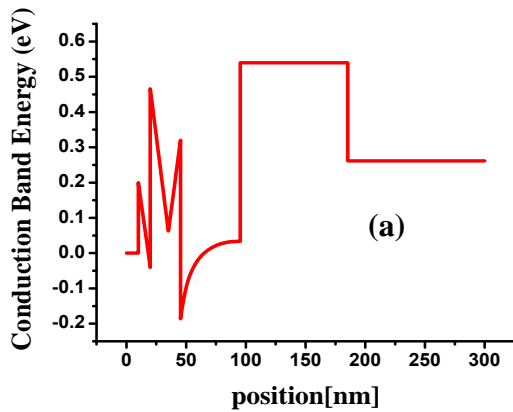
$$f_T = \frac{g_m}{2\pi C_{gs}} = \frac{v_{sat}}{2\pi L_g} \quad (6)$$

where  $C_{gs}$  is the gate to source capacitance,  $v_{sat}$  is the saturation carrier velocity in the channel and  $L_g$  is the gate length. The equation eqn-6 shows that improving saturation velocity and down-scaling gate length are the basic approaches to increase  $f_T$  [15].

#### 4. Results and Discussion

##### 4.1 Simulated Conduction Band Discontinuity ( $\Delta E_c$ ) and 2DEG of InP-Based HEMT

Double $\delta$ -doped InP-basedInAlAs/InGaAs lattice matched HEMT structure model is shown in Fig. 1. The simulated band structure of the conduction band ofInP-basedInAlAs/InGaAs HEMT due to single  $\delta$ -doping and double  $\delta$ -doping are shown in Fig. 2-a, Fig. 2-c respectively. The 2DEG or quantum well due to single  $\delta$ -doping and double  $\delta$ -doping are shown in Fig. 2-b and Fig. 2-d respectively, which is formed at the interface ofInGaAs and InAlAs due to their bandgap difference. From the simulation results, we observe that the carrier density is found to be very high at the wide band gap and narrower band gap material heterointerface. Also from simulation results very high carrier density is found at a distance of 55.3 nm to 105.3 nm. The electron density of this channel layer consists approximately  $1.8 \times 10^{18}/cm^3$  due to 1<sup>st</sup> $\delta$ -doping,  $2 \times 10^{18}/cm^3$  due to 2<sup>nd</sup> $\delta$ -doping.The electron transfer from both sides into the channel layer due to this channel layer consist the carrier density approximately  $1.8 \times 10^{18}/cm^3$  and  $2 \times 10^{18}/cm^3$  respectively due to double  $\delta$ -



doping which is quite high. A small amount (negligible) of the electron is found across  $\delta$ -doped layer because it is highly doped.

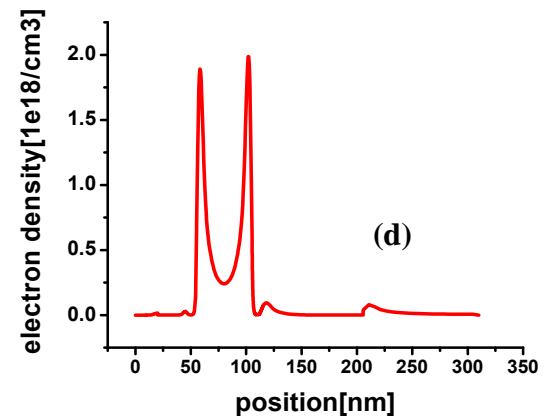
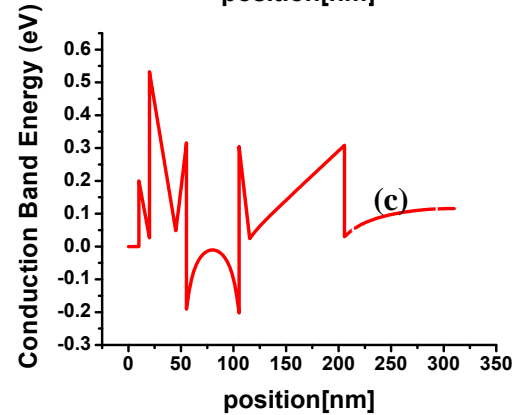
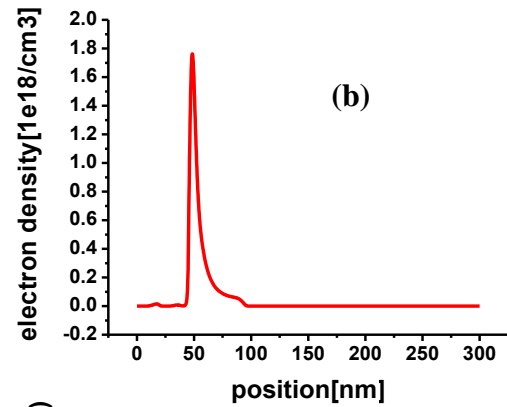


Figure 2:Conduction Band Energy, Carrier Concentration and band bending due to doping concentration. (a) Simulated Conduction Band Energy Diagram with position and Band Bending,  $\Delta E_c=0.5eV$  due to 1<sup>st</sup> $\delta$ -doping. (b) Simulated Plot of Electron Density (2DEG) Vs position due to 1<sup>st</sup> $\delta$ -doping. (c) Simulated Conduction Band Energy Diagram with position and Band Bending,  $\Delta E_c=0.5 eV$  due to 1<sup>st</sup> and 2<sup>nd</sup> $\delta$ -doping. (d) Simulated Plot of Electron Density Vs position due to 1<sup>st</sup> and 2<sup>nd</sup> $\delta$ -doping.

#### 4.2 Effect of $\delta$ -Doping ( $N_D$ ) Variation on device performance

From the simulation results it is found that as the electron concentration of  $\delta$ -doped layer increases, the carrier concentration in the channel layer also increases. In this HEMT device, we add two silicon  $\delta$ -doped layer. The simulation result of  $\delta$ -doping with electron density is shown in Fig.4-a. Further, from simulation result, we observe that initially the carrier concentration (2DEG) in the channel layer is raised linearly up to delta doping concentration of  $4.5 \times 10^{18} \text{ cm}^{-2}$ , any further increase in delta doping concentration, the electron density in the channel remains almost constant. Fig.4-b shows the simulation result of the variation of double  $\delta$ -doping concentration ( $N_D$ ) with threshold voltage ( $V_{th}$ ). However, from the simulation result it is found that threshold voltage of the device is shifted towards more negative as the 1<sup>st</sup> and 2<sup>nd</sup>  $\delta$ -doping concentration increases. Furthermore, the simulation result of  $\delta$ -doping concentration ( $N_D$ ) with transconductance ( $g_m$ ) is shown in Fig.4-c. From this simulation, it is found that the transconductance increases as the  $\delta$ -doping concentration increases, because drain current is increases. Also from this simulation it is found that a high transconductance peak at high  $N_D$ . Also, the effect of  $\delta$ -doping concentration ( $N_D$ ) on cut-off frequency ( $f_T$ ) is shown in Fig.4-d. The simulation result it is found that the Cut-off frequency is increases as the  $\delta$ -doping concentration increases. In this analysis, the current gain cut-off frequency 61.7 GHz is found at  $1 \times 10^{19} \text{ cm}^{-3}$   $\delta$ -doping concentration.

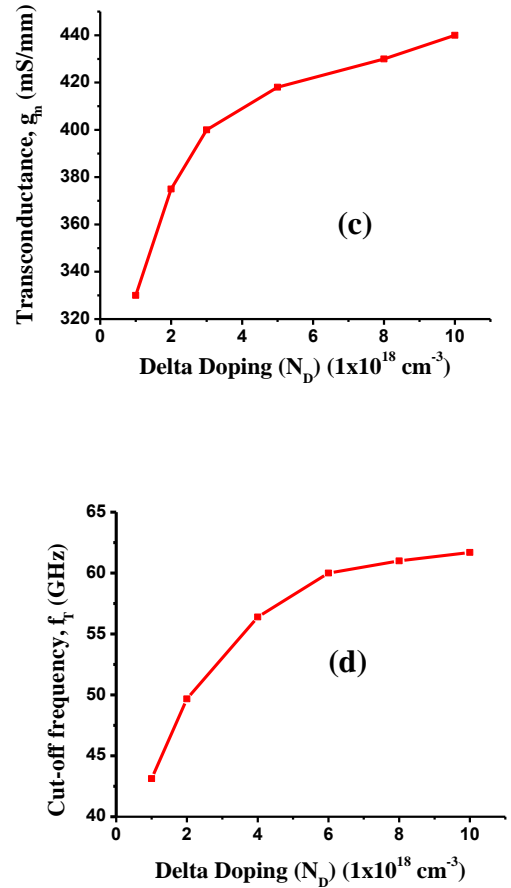
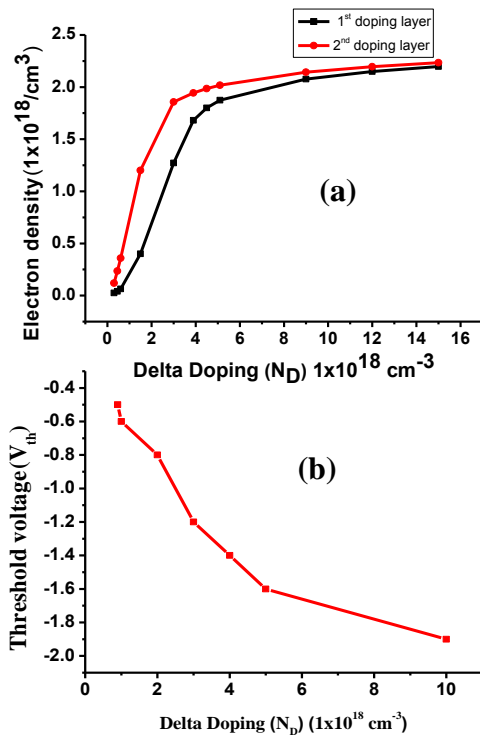


Figure 3: Effect of  $\delta$ -doping ( $N_D$ ) Variation. (a) Variation of 2DEG electron density with 1<sup>st</sup> and 2<sup>nd</sup>  $\delta$ -doping ( $N_D$ ). (b) Variation of threshold voltage ( $V_{th}$ ) with double  $\delta$ -doping ( $N_D$ ). (c) Variation transconductance ( $g_m$ ) with  $\delta$ -doping ( $N_D$ ). (d) Variation of cut-off frequency ( $f_T$ ) with  $\delta$ -doping ( $N_D$ ).

#### 4.3 Effect of Spacer Layer Thickness Variation on device performance

The spacer layer thickness plays an important role on the device performance. A thinner spacer layer thickness rises the total sheet carrier concentration into the InGaAs channel layer. However, a wider spacer layer rises the electron mobility in the channel but, decreases the carrier transfer efficiency in the channel. Further, the spacer layer separates the ionized donor ions from 2DEG, decreasing the Coulomb scattering with the donor ions and raise the electron mobility. The variation of 2DEG electron density in HEMT with a spacer layer thickness  $d_s$  is shown in Fig. 4-a. In Fig. 4-a also shows that the effect of channel concentration due to 1<sup>st</sup> doping and 2<sup>nd</sup> doping with spacer layer variation. The variation of spacer layer thickness also affects the threshold voltage  $V_{th}$ . This variation of threshold

voltage due to the spacer layer thickness is shown in Fig. 4-b.

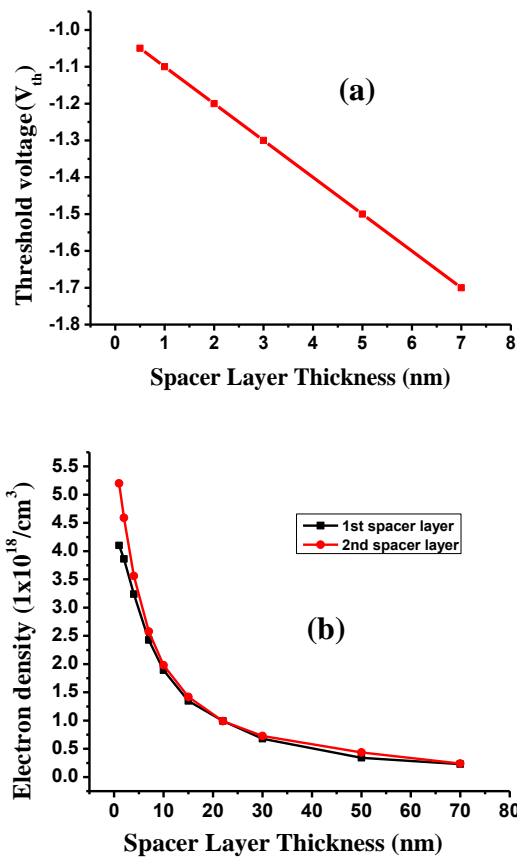
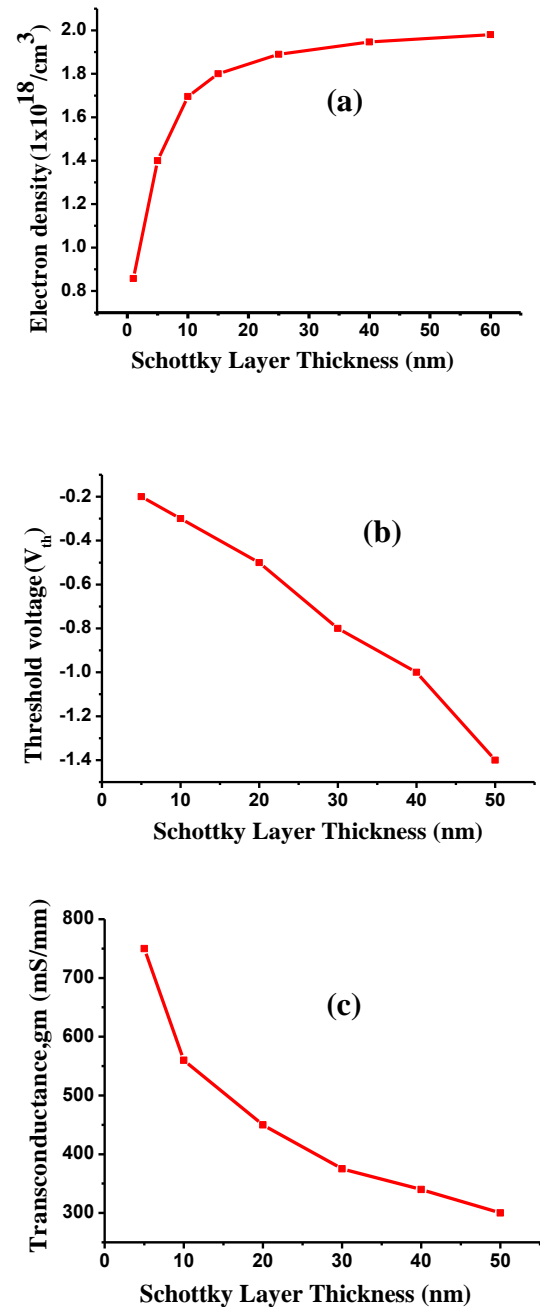


Figure 4: Spacer layer thickness variation. (a) Variation of 2DEG electron density with 1<sup>st</sup> and 2<sup>nd</sup> spacer layer thickness ( $d_s$ ). (b) Variation of threshold voltage ( $V_{th}$ ) with spacer layer thickness ( $d_s$ ).

#### 4.4 Effect of Schottky Layer Thickness Variation on device performance

In the HEMT device, the Schottky layer is a wide bandgap material where the channel layer a low bandgap material. Due to this high bandgap difference at the InAlAs/InGaAs heterointerface, where free carrier diffuses from higher bandgap InAlAs to lower bandgap InGaAs material to form 2DEG, which allows higher carrier sheet density and improve the carrier confinement into the channel. The effect of the variation of Schottky layer thickness on carrier concentration due to 1<sup>st</sup>  $\delta$ -doping is shown in Fig. 5a. In the simulation analysis, it is found that as the Schottky layer thickness increases the carrier concentration into the channel also increases linearly up to a certain limit then sub-linearly and finally saturated. However, a stripper Schottky layer decreases the distance

between the metal gate and channel, provide better gate control and improves the transconductance of the device but reduces the breakdown voltage. Also, the simulation result of Schottky layer thickness variation with a threshold voltage is shown in Fig. 5b. From this simulation result, it is observed that the threshold voltage of the device shifted towards more negative with increasing the Schottky layer thickness. Further, the effect of Schottky layer thickness variation on transconductance is shown in Fig. 5c. From this result, it is found that as the Schottky layer thickness decreases the transconductance of the device increases



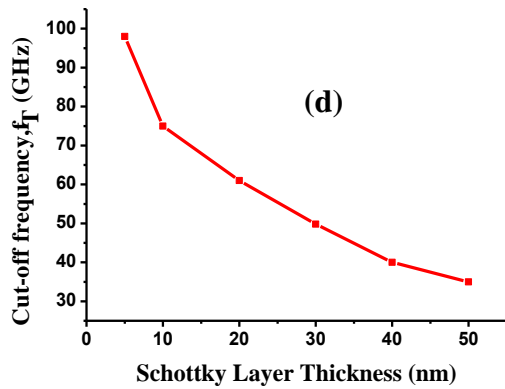


Figure 5: Schottky layer thickness ( $d_i$ ) variation. (a) Variation of 2DEG electron density due to  $1^* \delta$ -doping with Schottky layer thickness ( $d_i$ ). (b) Variation of threshold voltage ( $V_{th}$ ) with Schottky layer thickness ( $d_i$ ). (c) Variation transconductance ( $g_m$ ) with Schottky layer thickness ( $d_i$ ). (d) Variation cut-off frequencies ( $f_T$ ) with Schottky layer thickness ( $d_i$ )

because the threshold voltage decreases. Further, as the Schottky layer thickness decreases the current gain cut-off frequency is also rises. Effect of Schottky layer thickness variation on unity gain cut-off frequency is shown in Fig. 5d. In this simulation analysis, 98 GHz unity gain cut-off frequency is found at 5nm Schottky layer thickness.

#### 4.5 Effect of Gate Length ( $L_g$ ) Variation

The performance of HEMT enhanced with decreases the dimensions, especially the gate length as we consider the ballistic transport. Optimization of the device performance, like current gain cut-off frequency, can be done by varying the gate length [16]. The effect of the variation of threshold voltage with gate length is shown in Fig. 6a. The simulation result shows that as the gate length increases the threshold voltage of device decreases. However, as the gate length

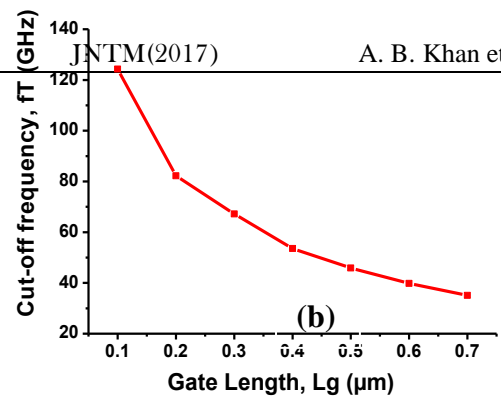
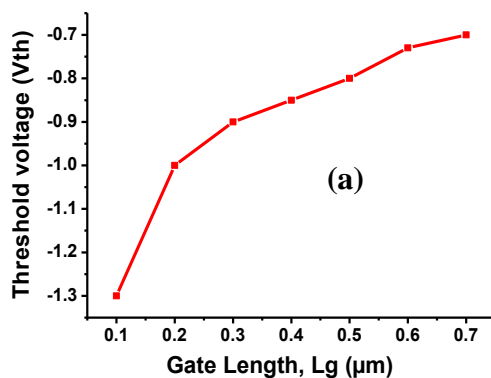


Figure 6: Effect of Gate length ( $L_g$ ) variation. (a) Variation of threshold voltage ( $V_{th}$ ) with gate length ( $L_g$ ). (b) Variation of cut-off frequency ( $f_T$ ) with gate length ( $L_g$ ).

decreases the current gain cut-off frequency is increased. The effect of gate length on the current gain cut-off frequency of the device is shown in Fig. 6b.

## 5. Conclusion

The optimization of 0.5  $\mu\text{m}$  gate length of InP-based InAlAs/InGaAs HEMT is done after varying some parameters. These parameters are spacer layer thickness ( $d_s$ ),  $\delta$ -doping concentration ( $N_D$ ), Schottky layer thickness ( $d_i$ ) and gate length ( $L_g$ ) which are used to optimize the device performance. Spacer layer is used to improve in the mobility of the channel. With the variation of double  $\delta$ -doping, the enhancement of device characteristics like channel concentration using  $\delta$ -doped through numerous contours of sheet carrier density, threshold voltage has been studied. The double delta doped HEMT is providing higher 2DEG density and higher transconductance than single doped HEMT. Further the device performance with Schottky layer thickness variation is also observed. When the Schottky layer thickness reduces, the threshold voltage becomes less negative due to this the transconductance and current gain cut-off frequency are increasing. Reduction on the device geometry like gate length, it is observing that the device performance is also affecting. Furthermore, the influence of the gate length variation on current the gain cut-off frequency and threshold voltage is also observed. The maximum cut-off frequency 125 GHz is observed at 5nm Schottky layer thickness, 0.1  $\mu\text{m}$  gate length and 1nm, spacer layer thickness.

## References

- [1] L. D. Nguyen, L. E. Larson, and U. K. Mishra, in *IEEE Proceedings*, vol. 80, pp. 494–518, 1992.
- [2] K. Joshin, T. Kikkawa, S. Masuda, and K. Watanabe, *Fujitsu Sci. Tech. J.*, vol. 50, no. 1, pp. 138–143, 2014.

- [3] Lepore A., Levy M., Lee H., Kohn E., Radulescu D., Tiberio R., Tasker P., Eastman L., *Electron Devices, IEEE Transactions*, Vol. 35, No. 12, pp. 2441 - 2442, Dec 1988
- [4] K. Shinohara, Y. Yamashita, A. Endoh, I. Watanabe, K. Hikosaka, T. Matsui, T. Mimura, and S. Hiyamizu, *IEEE Electron Device Lett.*, Vol. 25, No. 5, May 2004.
- [5] S. Gupta, F. Rahman, M. J. Siddiqui, and P. A. Alvi, "Strain profile in nitride based multilayer nano-heterostructures," *Phys. B Phys. Condens. Matter*, vol. 411, pp. 40-47, 2013.
- [6] P. A. Alvi, S. Gupta, M. J. Siddiqui, G. Sharma, and S. Dalela, "Modeling and simulation of GaN/Al<sub>0.3</sub>Ga<sub>0.7</sub>N new multilayer nano-heterostructure," *Phys. B Phys. Condens. Matter*, vol. 405, no. 10, pp. 2431-2435, 2010.
- [7] P. A. Alvi, S. Gupta, P. Vijay, G. Sharma, and M. J. Siddiqui, "Affects of Al concentration on GaN/AlGa<sub>0.3</sub>N new modeled multilayer nano-heterostructure," *Phys. B Phys. Condens. Matter*, vol. 405, no. 17, pp. 3624-3629, 2010.
- [8] D. Delagebeaudeuf and N. T. Linh, *Electron Devices, IEEE Transactions on*, vol. 29, no. 6, pp. 955-960, 1982.
- [9] Farhan Aziz, M.J. Siddiqui, International Journal of Emerging Technologies in Computational and Applied Science, Vol. 4, No. 1, pp. 42-48, March-May, 2013.
- [10] F. Aziz, M. Siddiqui, and M. Khan, in International Conference on Electronics Information and Communication Systems Engineering (ICEICE-2010).
- [11] R. Gupta, S. K. Aggarwal, M. Gupta, and R. Gupta, *Journal of semiconductor Technology And Science*, vol. 4, no. 3, pp. 240-249, 2004.
- [12] L. Aina, M. Burgess, M. Mattingly, J. M. O'Connor, A. Meerschaert, M. Tong, A. Ketterson, and I. Adesida, *Electron Device Letters, IEEE*, vol. 12, no. 9, pp. 483-485, 1991.
- [13] S. N. Mohammad and H. Morkoc, *Compound Semiconductor Electronics: The Age of Maturity*, p. 25, 1996.
- [14] S. M. Sze, New York, Wiley-Interscience, 1990, 653 p. *No individual items are abstracted in this volume.*, vol. 1, 1990.
- [15] N. Waldron, D.-H. Kim, J. del Alamo, et al., *Electron Devices, IEEE Transactions on*, vol. 57, no. 1, pp. 297-304, 2010
- [16] A. B. Khan, M. Siddiqui, M. M. Singh, and C. Thaseena, in Multimedia, Signal Processing and Communication Technologies (IMPACT), 2013 International Conference on, pp. 264-267, IEEE, 2013.